

TRADEOFFS ASSOCIATED WITH SEDIMENT-MAINTENANCE FLUSHING FLOWS: A SIMULATION APPROACH TO EXPLORING NON-INFERIOR OPTIONS

FU-CHUN WU^{a*} and YI-JU CHOU^b

^a *Department of Bioenvironmental Systems Engineering and Hydrotech Research Institute National Taiwan University, Taipei 106, Taiwan, Republic of China*

^b *Department of Bioenvironmental Systems Engineering National Taiwan University, Taipei 106, Taiwan, Republic of China*

ABSTRACT

Sediment-maintenance flushing flows designed to mimic the action of natural floods in removing the accumulated fine sediments from the channel and loosening the gravel bed have been increasingly proposed as an effective alternative in dam management and a required component of riverine restoration programmes. However, reservoir releases are generally associated with financial and environmental costs, thus it is highly desirable to specify flushing flows as accurately as possible. In this paper we present a simulation approach to evaluating flushing flows and exploring the tradeoffs associated with non-inferior flushing options. A two-fraction sediment routing model is used to simulate the gravel-sand bed response to flushing flows. The results reveal that the sand cleansing effect propagates from upstream to downstream and from surface to subsurface. Under a steady gravel supply from upstream, an equilibrium state of gravel transport and bed degradation is eventually reached in the simulation reach. The flushing flow and sediment transport system investigated in this study involves a transient state variable (bed sand content), a decision variable (flushing flow discharge), a flushing goal (ultimate bed sand content), and three outcomes to be minimized (flushing duration, released water volume, and total gravel loss). A series of numerical simulations are carried out with a range of flows and pre-flushing bed sediment conditions. The results reveal that the flushing efficiency is higher for the larger flow. However, for flows greater than $\sim 100 \text{ m}^3/\text{s}$ the flushing duration is less sensitive to the flow discharge, thus the system may be simplified as a bi-objective one. The gravel loss and water volume are two conflicting outcomes within the non-inferior flow region. Under a worse bed sediment condition, the feasible flushing options are constrained in a narrower range and also associated with higher costs. The tradeoffs between the conflicting outcomes are quantitatively displayed with the transformed feasible solutions in the objective space. We provide here a general and practical approach permitting a quantitative evaluation of the different flushing options that is appropriate to the level of data typically available. Copyright © 2004 John Wiley & Sons, Ltd.

KEY WORDS: model simulation; flushing flow; sediment maintenance flow; multi-objective system; tradeoff; non-inferior option; decision analysis

INTRODUCTION

Flushing flow releases have been increasingly proposed as an effective alternative in dam management and a required component of riverine restoration programmes (Milhous, 1982; Reiser *et al.*, 1989; Ligon *et al.*, 1995). Such controlled flow releases designed to mimic the action of natural floods in removing the accumulated fine sediments from the channel and loosening the gravel bed are categorized as ‘sediment maintenance flows’, which are generally smaller in magnitude than the other category, termed ‘channel maintenance flows’, intended to maintain the channel and floodplain geometry (Andrews and Nankervis, 1995; Kondolf and Wilcock, 1996). Releases of sediment-maintenance flushing flows are important for mitigating the adverse effects caused by the intrusion of fine sediment into gravel beds, in particular the degraded quality of salmonid spawning gravels (Reiser, 1998; Wu, 2000). Sand-free gravel beds are a key element for egg and embryo development and thus a major driver of this type of management action. Planning of the sediment maintenance flows needs to specify the magnitude,

* Correspondence to: Fu-Chun Wu, Department of Bioenvironmental Systems Engineering and Hydrotech Research Institute, National Taiwan University, Taipei 106, Taiwan, Republic of China. E-mail: fcwu@hy.ntu.edu.tw

duration, and timing of the flow releases. Some practical guidelines have been proposed. For example, Reiser *et al.* (1989) pointed out several factors to be incorporated in determination of the best time for implementing a sediment maintenance flow, which include the life-history requirements of the target species, historical runoff period, and flow availability. Wilcock (1998) noted that typically in the USA the timing and the rate of change of reservoir release are based entirely on the ecological requirements of the stream biota. Moreover, Milhous (1982) suggested that the timing of flushing flow releases during the incubation period of fish eggs should depend upon the survival rate to be maintained; accordingly Wu (2000) incorporated an embryo survival model to prescribe the preferred timing of flow releases. Despite these specific criteria for the best timing, determination of the magnitude and duration of a sediment maintenance flow involves a number of interactive factors, such as the bed sand content, water budget, and desired bed quality, that make the formulation of a method applicable to all stream systems for all purposes an extremely difficult task (Reiser *et al.*, 1989). Therefore, it is not surprising that broad rules based on simple analogy are often used in the planning of flushing flows (Wilcock *et al.*, 1996b).

However, reservoir releases are generally associated with financial and environmental costs, such as the lost power generation, reduced water supply, and loss of spawning gravels to the downstream (Kondolf and Wilcock, 1996). Thus, it is highly desirable to specify flushing flows as accurately as possible so that the unnecessary costs can be minimized. Figure 1 depicts the interrelations between the components involved in a flushing flow and sediment transport (flow-transport) system. It shows that the duration of a flushing flow (labelled as Objective 1) is directly governed by the flushing goal (i.e. the quantity of sand to be removed) and the sand transport rate. Of these two governing factors, the former corresponds to the bed sand content (a transient state variable, connected by a dashed line) and the desired bed quality (or the maximum acceptable sand content); the latter is a complex function of flow discharge (labelled as a decision variable), implying that the flushing duration indirectly relies on the magnitude of flushing flow. Supposing that the duration for achieving the flushing goal can be determined, the released water volume (labelled as Objective 2) is simply evaluated by the product of flow discharge and duration. Similarly, to estimate the gravel loss (labelled as Objective 3), one needs to calculate the difference between the total gravel output and input through a stream reach, which involves the integration of gravel transport rate over the

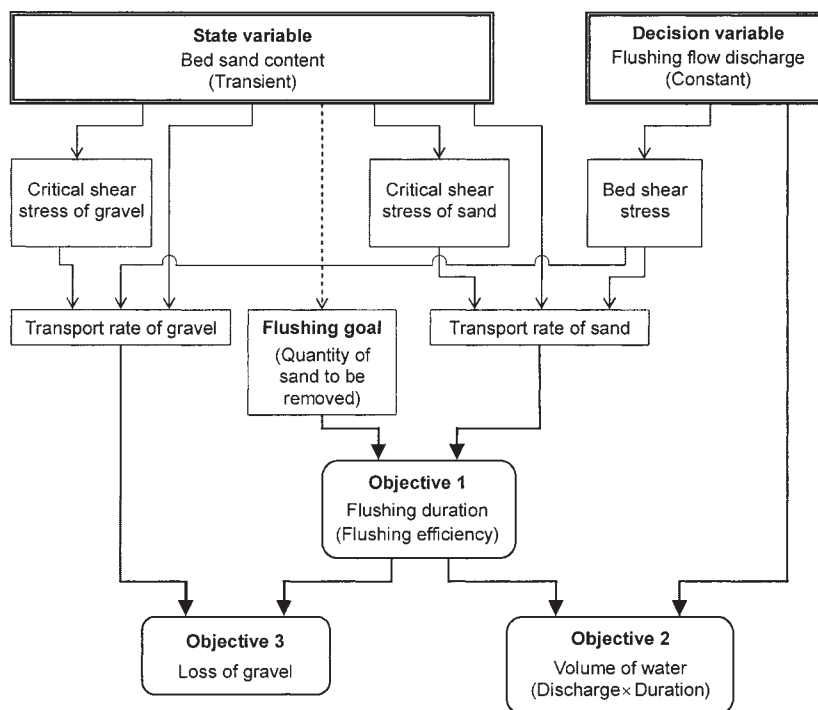


Figure 1. Interrelations between the components and outcomes involved in a flushing flow and sediment transport (flow-transport) system

flushing duration. For this multi-objective system, reliable estimations of all these interactive quantities are difficult to achieve without access to a suitable simulation model.

A simplified two-part sediment routing algorithm was developed for evaluating the removal of sand from a gravel bed by the flushing flow (Wilcock *et al.*, 1996b). However, the dependence of sediment entrainment thresholds on sand content and the bed degradation were not considered in their simplified model. Herein, we apply a recently developed two-fraction sediment routing model to the conditions of a representative gravel-bed river to explore the tradeoffs associated with specifying flushing flows. The evolutions of bed composition, bed elevation, and sediment transport rates induced by flushing flows are investigated. A series of numerical simulations are then carried out with a range of flows and bed sediment conditions. The simulation results are used as a basis for determining the non-inferior options, which are further transformed to the feasible options in the objective space for demonstration of the tradeoffs between the conflicting outcomes. We present in this paper a practical approach to quantitatively evaluating the different flushing options that is appropriate for the sparse field data typically accessible.

SIMULATION MODEL

A two-fraction sediment routing model is used to simulate the gravel-sand bed response to flushing flows. The model is more sophisticated than an earlier one (Wilcock *et al.*, 1996b), yet still simple enough for evaluation of flushing options. The model was developed for the depth flushing process and sufficient confirmation of this model has been provided by laboratory tests (Wu and Chou, 2003). The primary advance of this model is incorporation of a two-fraction entrainment approach into a routing framework to account for the effect of sand content f_s on the entrainment of bed sediment, which is crucial for simulation of the flushing process that is characterized by progressively decreasing f_s values. The two-fraction entrainment approach divides the bed sediment into two size fractions, i.e. sand (<2 mm) and gravel (>2 mm). From field and laboratory observations, it is found that the critical shear stresses for sand and gravel, τ_{cs} and τ_{cg} , linearly decrease with f_s in the region between 0.2 and 0.4, beyond which τ_{cs} and τ_{cg} remain constant (Wu and Chou, 2003).

Sediment routing computations are based on the mass conservation of sediment in both the surface and subsurface layers. Bedload transport mainly takes place in the surface layer. The entrainment of subsurface gravel would produce an upward sand flux from the subsurface (Wilcock *et al.*, 1996b). For a channel reach of length L , the total input of sediment to the surface layer in a time step Δt is the sum of bedload inflow from upstream and upward sand supply from subsurface. The former is evaluated by $(q_{bs,in} + q_{bg,in})\Delta t$, where $q_{bs,in}$ and $q_{bg,in}$ are the sand and gravel transport rates (mass/width/time) from upstream, while the latter is evaluated by $q_{sub,s}L\Delta t$, where $q_{sub,s}$ is the upward sand flux from the subsurface layer (mass/area/time), which can be expressed as:

$$q_{sub,s} = C_u \left(\frac{f_{ss} - f_s}{f_{ss}} \right) \frac{M_{ss}}{t_{ex}} \quad (1)$$

where f_s and f_{ss} = proportions of sand in the surface and subsurface layers, respectively; M_{ss} = mass of sand in the unit-area subsurface layer; t_{ex} = exchange time, is a timescale defined as the duration producing spatially complete gravel entrainment; the upward entrainment constant C_u is taken to be 0.5 (Wilcock *et al.*, 1996b). The total output of sediment from the surface layer equals the sum of sand and gravel outflows, as given by $(q_{bs,out} + q_{bg,out})\Delta t$, where $q_{bs,out}$ and $q_{bg,out}$ vary with the f_s value in that channel reach. The difference between the sediment input and output is the change of sediment storage in the surface layer.

Sediment routing computations are executed in two steps. First, the change of bed level is computed with the continuity equation of sediment in the surface layer:

$$(1 - \lambda) \frac{\partial H}{\partial t} = \frac{1}{\rho_s} \left(-\frac{\partial q_T}{\partial x} + q_{sub,s} \right) \quad (2)$$

where H = bed level elevation; λ = effective porosity of surface layer; ρ_s = density of sediment; q_T = total bedload transport rate; x = streamwise distance; t = time. When the bed level is lowered (or raised) by an amount of

ΔH in a time step Δt due to degradation (or aggradation), the boundaries of the surface and subsurface layers are shifted downward (or upward) accordingly, such that the thickness of the surface and subsurface layers remains invariant. Second, the changes of sediment storage in the surface and subsurface layers are computed with the mass conservations of sediment. In addition to the bedload difference between the upstream inflow and downstream outflow, the upward sand entrainment from subsurface is added to the storage of sand in the surface layer but removed from the storage of sand in the subsurface layer. Given the bed level change, the quantities of sand and gravel in the shifted surface and subsurface layers can be re-evaluated. Then the corresponding f_s and f_{ss} values are updated at the end of each time step (see Wu and Chou (2003) for more details).

MODEL PARAMETERS

Study site

Parameter values for the Trinity River in northern California, USA (Figure 2), are used as representative values of many gravel-bed rivers (Wilcock *et al.*, 1996a,b). The study site is located downstream of the Lewiston Dam (impounded since 1961). Flow regulation has reduced the discharge (e.g. mean annual flood reduced from 525 to 73 m³/s) and sediment transport capacity in the mainstem, while sediment yields from the tributaries have increased as a result of road construction and timber harvest. Most notable is the Grass Valley Creek (~13 km downstream of the Lewiston Dam), which has caused significant accumulation of fine sediment in the Trinity River. It is reported that 90% of the Grass Valley Creek basin was logged during 1950–60, leading to estimated annual sediment yields of 102 000 m³ in the 1970s (Wilcock *et al.*, 1996b). The 2.7-km-long river reach downstream of the Grass Valley Creek confluence is our simulation reach (Figure 2). Constant-discharge trial releases from Lewiston Dam were made in 1991–93, providing opportunities for observing the flow–transport relations and channel bed evolutions (Wilcock *et al.*, 1996a). Measurements were made at Poker Bar, located 15 km downstream of the Lewiston Dam. The river channel near Poker Bar is constantly ~35 m wide and rectangular in shape; bank-full discharge of this reach is ~75 m³/s.

The size distributions of the bed materials taken before and after the 1992 release are shown in Figure 3. It is revealed that the pre- and post-flushing bed compositions were nearly identical (Figure 3a), indicating that the sand cleansing effect, which proceeds from upstream to downstream, did not reach Poker Bar after 5 days at 164 m³/s. The pre- and post-flushing sand proportions were both 0.19. Although the surface and subsurface materials were not separately sampled because of the turbidity (Wilcock *et al.*, 1996a), herein we take 0.19 as the background value of bed sand content. The fractional size distributions truncated at 2 mm size boundary (Figure 3b) indicate that the median sizes of the gravel and sand fractions, D_g and d_s , are 30 and 0.8 mm, respectively; D_{84} of the gravels (= surface layer thickness L_s) is 75 mm. The values of ρ_s , n_g and n_s are 2700 kg/m³, 0.23 and 0.17, respectively.

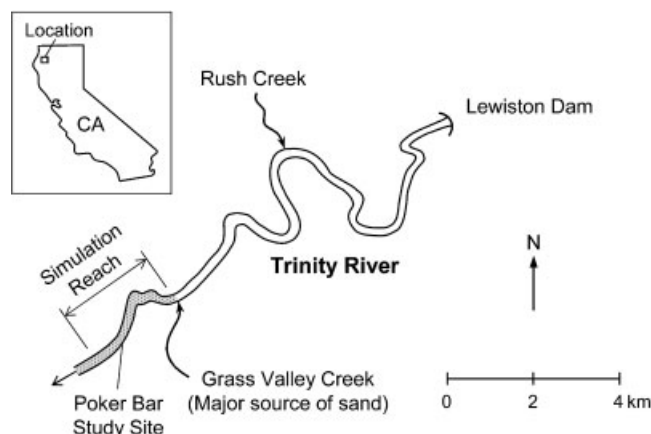


Figure 2. Location map of the Trinity River study site and Poker Bar simulation reach

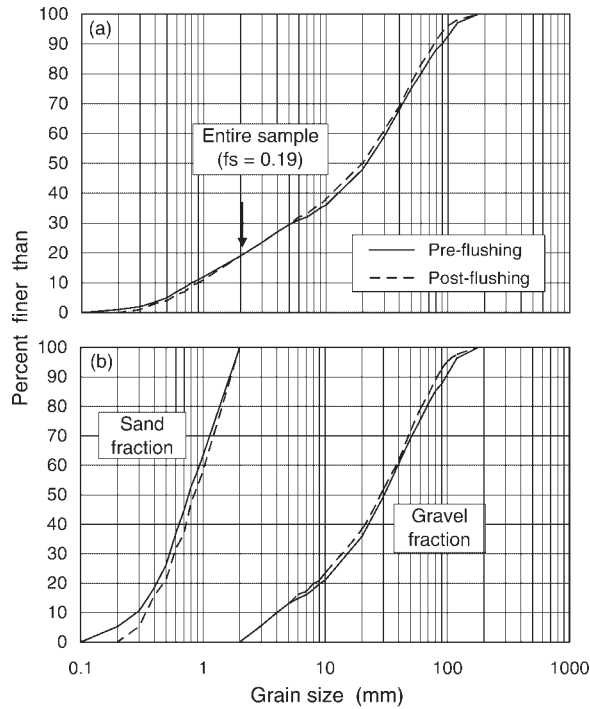


Figure 3. Grain size distributions of the bed material taken at Poker Bar study site before and after the 1992 trial release. (a) Entire size distributions. (b) Fractional size distributions truncated at 2 mm boundary

According to the observations at the study site, the active layer thickness (= the depth of gravel entrainment) increased with the bed shear stress τ_0 . An empirical relation was proposed for evaluation of the active layer thickness L_a (Wilcock *et al.*, 1996a):

$$L_a = 1.7(1 - 0.031/\tau_g^*)^{0.26}D_{84} \tag{3}$$

where the Shields stress $\tau_g^* = \tau_0/(\gamma_s - \gamma)D'_g$, $D'_g = 36$ mm; γ_s and γ = specific weights of sediment and water, respectively. The surface layer thickness D_{84} is used in Equation 3 as a scaling length. From Equation 3, the limiting value of L_a is $1.7D_{84}$ as τ_0 becomes sufficiently large. The maximum depth of sand removal, $L_s + L_{ss}$ ($= 2D_{84}$), is slightly greater than the maximum L_a ($= 1.7D_{84}$) by $0.3D_{84}$, which can be generalized as $L_s + L_{ss} = L_a + 0.3D_{84}$. Given $L_s = D_{84}$, one can evaluate the thickness of subsurface layer as $L_{ss} = L_a - 0.7D_{84}$, in which L_a is evaluated from Equation 3 for the given τ_0 . These values of L_s and L_{ss} are required for defining the boundaries of the surface and subsurface layers.

Bedload transport rates

Bedload measurements were made at Poker Bar in 1992 and 1993 (Wilcock *et al.*, 1996a). After careful analyses, we obtain a set of predictive equations for sand and gravel transport rates:

$$q_{bs} = 0.625f_s(1 - \tau_{cs}/\tau_0)^{0.356} \quad \text{for } f_s \leq 0.2 \tag{4a}$$

$$q_{bs} = 0.125(1 - \tau_{cs}/\tau_0)^{0.356} \quad \text{for } f_s \geq 0.2 \tag{4b}$$

$$q_{bg} = 0.0018\tau_0^{1.5}(1 - \tau_{cg}/\tau_0)^{0.459} \quad \text{for } f_s \leq 0.4 \tag{4c}$$

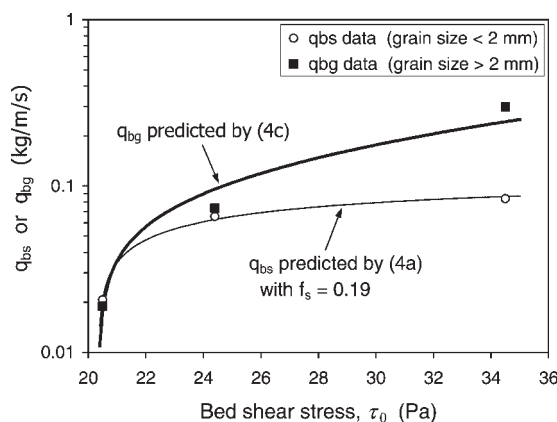


Figure 4. Gravel and sand transport rates as a function of bed shear stress

where q_{bs} and q_{bg} are in kg/m/s; τ_{cs} , τ_{cg} , and τ_0 are in Pa. The predicted bedload transport rates coincide well with the data extracted from Wilcock *et al.* (1996a), as shown in Figure 4. To use Equation 4, the values of f_s , τ_{cs} or τ_{cg} , and τ_0 are needed. Herein a value of 0.19 is used for f_s ; the value of τ_{cs} or τ_{cg} for the given f_s is estimated with the two-fraction entrainment thresholds (Wu and Chou, 2003). The local bed shear stress τ_0 can be determined with the following empirical relation:

$$\tau_0 = 0.166Q + 7.22 \quad (5)$$

where τ_0 is in Pa; Q is flow discharge in m^3/s .

Upward sand entrainment rate

To evaluate the upward sand entrainment rate $q_{sub,s}$ with Equation 1, the exchange timescale t_{ex} is needed. A trial release of $164 m^3/s$ for 5 days in 1992 was observed to produce nearly complete entrainment of the bed surface. With this as a reference combination of Q and minimum duration, one can use the gravel transport rate given by Equation 4c to evaluate t_{ex} (in days) for other Q values that produce the same volume of gravel transport (Wilcock *et al.*, 1996b), i.e.

$$t_{ex} = 5(q_{bg,92}/q_{bg}) \quad (6)$$

where $q_{bg,92}$ = gravel transport rate corresponding to the 1992 trial release (calculated with $Q = 164 m^3/s$, $f_s = 0.19$); q_{bg} = gravel transport rate evaluated for other Q and f_s values.

Simulation conditions

A numerical simulation is carried out to investigate the temporal and spatial variations of bed composition, bed elevation, and sediment transport rates associated with the release of flushing flow at $Q = 100 m^3/s$. The simulation reach is divided into three sub-reaches (each with $L = 900 m$) designated as 1 to 3 from upstream to downstream. Given that Grass Valley Creek is the major source of sand to the Trinity River, and Lewiston Dam entraps the upstream incoming fine sediment, the river reach between Lewiston Dam and the Grass Valley Creek confluence is assumed to contain very little sand (i.e. $f_s \approx 0$) such that practically no sand is conveyed to the simulation reach from upstream. Also hypothesized is that this upstream reach, 13 km in length, is sufficiently long to provide a steady gravel supply. This upstream gravel supply rate ($= 0.0874 kg/m/s$) is estimated with Equation 4c using the τ_0 and τ_{cg} values determined for the given Q and f_s . The pre-flushing values of f_s and f_{ss} in the entire simulation reach are taken to be 0.28 and 0.19, respectively. The flushing duration is specified such that the simulation is terminated when $f_s \leq 0.05$ is met in all sub-reaches. The t_{ex} value is estimated with Equation 6 for the given Q and f_s . The time step Δt used here is 1 min, which is less than 0.1% of the flushing duration.

SIMULATION RESULTS AND DISCUSSION

Surface sand content and sand transport rate

The evolutions of surface sand content within sub-reaches 1–3 (Figure 5a) demonstrate clearly the downstream propagation of the sand cleansing effect. For example, sub-reach 1 reaches $f_s = 0.2$ in 2.6 days, while sub-reach 3 reaches this value in 14.7 days. Also, it takes 12.9 days to achieve $f_s \leq 0.05$ in sub-reach 1, while it takes 37.7 days to meet this criterion in sub-reach 3. This downstream propagation of sand cleansing effect leads to the

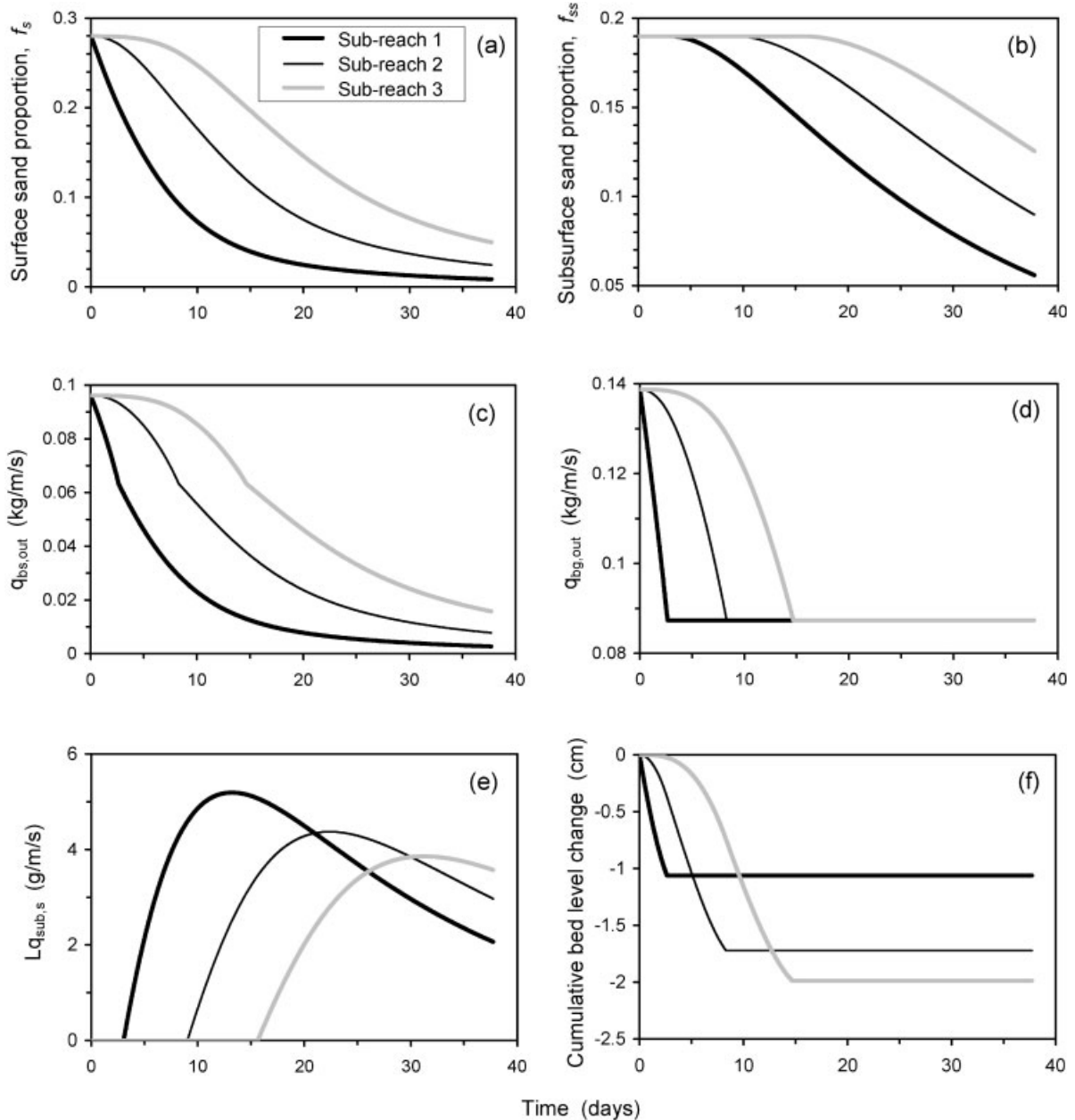


Figure 5. Simulated temporal–spatial variations of: (a) surface sand proportion; (b) subsurface sand proportion; (c) sand transport rate; (d) gravel transport rate; (e) upward sand entrainment rate from subsurface; (f) cumulative bed level change (simulation conditions: $Q = 100 \text{ m}^3/\text{s}$, pre-flushing $f_s = 0.28$)

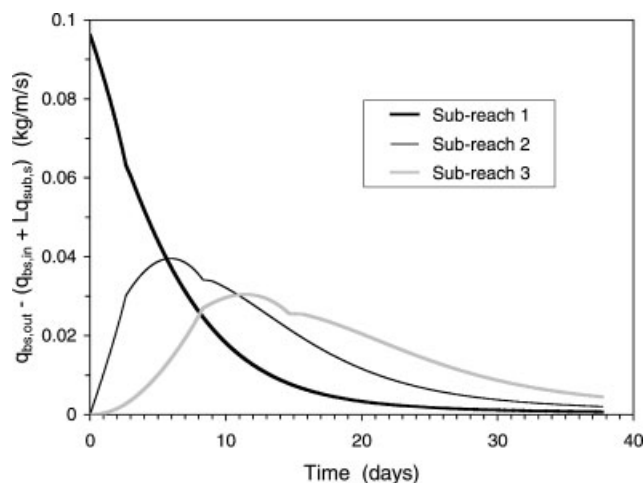


Figure 6. Temporal-spatial variations of net sand removal rate (calculated with the results shown in Figure 5)

development of downstream increasing sand transport rate (Figure 5c). The breaks in slope in Figure 5c are attributed to the transition from sand transport equation 4b to 4a, which takes place when the f_s value is reduced to 0.2, occurring in sub-reaches 1–3 after 2.6, 8.3 and 14.7 days of flow release, respectively. The declining trend of the sand transport rate is steeper prior to the transition but becomes much milder at the end.

From the mass conservation of sand in the surface layer, the rate of net sand removal from a sub-reach can be evaluated with the difference between the sand output $q_{bs,out}$ and total sand input ($q_{bs,in} + Lq_{sub,s}$). The evolutions of the rate of net sand removal from sub-reaches 1–3 (Figure 6) quantitatively demonstrate the downstream propagation of sand cleansing effect. The rate of net sand removal from sub-reach 1 shows a sharp declining trend, which is reduced to half the initial value in 4.5 days. The net sand removal rate of sub-reach 2 increases rapidly at the beginning and exceeds that of sub-reach 1 at 5.6 days. Shortly thereafter, the net sand removal rate of sub-reach 2 starts to decline. The net sand removal rate of sub-reach 3 increases slowly, but exceeds that of sub-reach 2 at 10.9 days and starts to decrease thereafter. The variation pattern illustrated in Figure 6 is similar to the downstream propagation of the maximum upward sand entrainment rate shown in Figure 5e, except that the rate of net sand removal from sub-reach 1 is initially at its maximum value.

Subsurface sand content and upward sand entrainment

In contrast to the prompt response of surface sand content to the flushing flow release, the temporal variations of subsurface sand content (Figure 5b) demonstrate substantial delays in the initiation of sand removal. The f_{ss} values in sub-reaches 1–3 remain at the initial level ($=0.19$) for 3, 9 and 15.6 days, respectively. The subsurface sand content starts to decline after the onset of upward entrainment. The upward sand entrainment from subsurface, as given by Equation 1, is driven by $(f_{ss} - f_s)$, which becomes effective as f_s is reduced to 0.19 (Figure 5a and e). Once initiated, the upward sand entrainment rate rapidly reaches the maximum value ($=5.2, 4.4$ and 3.9 g/m/s for sub-reaches 1–3, respectively) and then declines more slowly. Although the values of $Lq_{sub,s}$ decrease after the peaks (Figure 5e), the declines of $q_{bs,in}$ (Figure 5c) are much faster than those of $Lq_{sub,s}$ such that the contribution of subsurface sand entrainment to the total surface sand inflow still increases. At the end of simulation ($=37.7$ days), the contributions of subsurface sand to the total surface sand inflow of sub-reaches 2 and 3 exceed 50 and 30%, respectively. Eventually, the subsurface sand cleansing will dominate over the surface sand cleansing, which is well demonstrated by the much greater decreasing trends of f_{ss} than those of f_s near the end of simulation (Figure 5a and b). In summary, these results indicate that the sand cleansing effect propagates from upstream to downstream, and from surface to subsurface.

Gravel transport rate and bed level change

The evolutions of gravel transport rate (Figure 5d) reveal that $q_{bg,out}$ decreases rapidly at the beginning but eventually reaches equilibrium. Prior to the equilibrium, the gravel transport rate declines over time because of the

progressively elevated τ_{cg} value resulting from the decreasing f_s . For $f_s \leq 0.2$, τ_{cg} is constant and thus the gravel transport rate remains at equilibrium ($= 0.0874 \text{ kg/m/s}$). However, due to the downstream propagation of sand cleansing effect, the equilibrium gravel transport is also achieved from upstream to downstream. As the equilibrium state is reached in a sub-reach, the gravel inflow is balanced by outflow and thus the reach-averaged bed elevation remains unchanged. The cumulative bed level changes (Figure 5f) reveal that the equilibrium degradation depths in sub-reaches 1–3 are 1.1, 1.7 and 2 cm, respectively. The greatest degradation in sub-reach 3 is primarily due to the longest time needed to reach equilibrium. Degradation of the channel bed implies the potential loss of gravel to the downstream associated with the flushing flow releases.

A key question emerging here is that if degradation were primarily a function of flushing duration and the duration decreased with the increase of flushing flow discharge, would the degradation also reduce with the increase of flow discharge? Obviously, the answer to this question is not straightforward. The greater flow almost certainly increases the flushing efficiency (i.e. reduces the flushing duration), but the higher gravel transport rate associated with the larger flow would probably lead to greater degradation even though the flushing duration is shortened, and the resulting volume of water released is not necessarily a favourable outcome. Because the released water volume is the product of flow discharge and duration, the decrease in flushing duration must be relatively greater than the increase in flow discharge to ensure a reduced water volume. The tradeoffs among the interrelated outcomes can only be quantitatively investigated with the simulation results. In the following section, a series of flushing simulations are carried out with a range of flows and the results are used to explore the non-inferior options of this multi-objective system as well as the tradeoffs associated with different flushing options.

EVALUATION OF FLUSHING OPTIONS

For the flow-transport system depicted in Figure 1, the outcomes (Objectives 1–3) are substantially influenced by the bed-sediment condition (a state variable), the ultimate goal to be achieved (flushing goal), and the flushing flow discharge (a decision variable). Given the complexity of this system, it is unlikely that one can obtain specific equations to express the objectives as a simple function of decision and state variables. To systematically evaluate the flushing options under the given bed-sediment condition, a series of numerical simulations are carried out with a range of flows (85 to $200 \text{ m}^3/\text{s}$). This flow range is based on the observations that little transport of bed material occurred for $Q \leq 85 \text{ m}^3/\text{s}$ at the Trinity River study site (Wilcock *et al.*, 1996b). Because the bed sand content is a state variable that significantly affects the sediment transport rates and thus the flushing duration, five different values of pre-flushing f_s , ranging from 0.24 to 0.32 (typical values for the gravel-bed rivers in need of flushing), are used in the simulations. The flushing goal is specified to remove sand from the channel bed such that $f_s \leq 0.05$ is met in the entire simulation reach. The outcomes of this flow-transport system, including the flushing duration, released water volume, and total gravel loss, are discussed in the subsequent sections. The non-inferior options derived from these results are presented in the last section.

Flushing duration versus flow discharge

Variations of flushing duration with flow under various pre-flushing f_s values (Figure 7) reveal that the required flow duration to achieve the specified flushing goal decreases with the increase of flow discharge, i.e. the larger flow is more efficient in sand cleansing. For a given flow, it is shown that the flushing duration is longer under the higher pre-flushing f_s value. Although the flushing efficiency is higher for the greater flow, the marginal efficiency associated with the greater flow is considerably lower. For example, under the condition of pre-flushing $f_s = 0.32$, the required flushing duration is reduced by 11.5 days (from 51.5 to 40 days) as the flow increases from 85 to $100 \text{ m}^3/\text{s}$, whereas the duration is reduced by only 5 days (from 40 to 35 days) as the flow increases from 100 to $200 \text{ m}^3/\text{s}$. The marginal flushing efficiency for the range 100 – $200 \text{ m}^3/\text{s}$ is 93% lower than that for the range 85 – $100 \text{ m}^3/\text{s}$. For flows greater than $\sim 100 \text{ m}^3/\text{s}$, increasing the flow magnitude does not significantly increase the flushing efficiency. As such, for these greater flows, it is very unlikely that the flushing duration would be a major concern in the evaluation of flushing options. Assessment of these larger flows thus needs to examine other outcomes of the system.

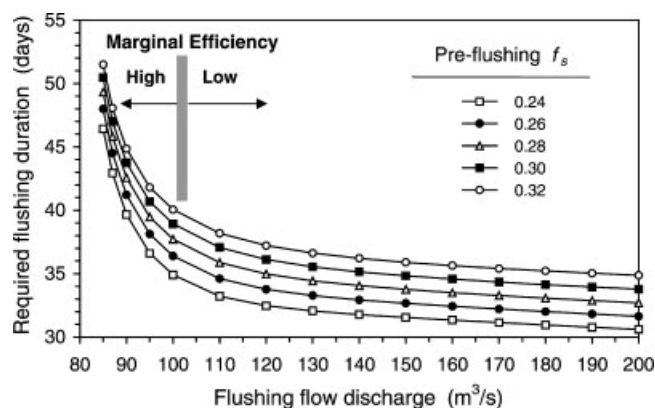


Figure 7. Variations of flushing duration with flushing flow discharge under different pre-flushing f_s values

Released water volume versus flow discharge

Variations of the released water volume as a function of flushing flow under five different pre-flushing f_s values (Figure 8) reveal that for $Q < \sim 95 \text{ m}^3/\text{s}$ the released water volume decreases with the increase in flow discharge. However, for $Q > \sim 100 \text{ m}^3/\text{s}$, the released water volume increases with flow discharge. Such trends can be explained with the results shown in Figure 7. For $Q < \sim 95 \text{ m}^3/\text{s}$ the decline in flushing duration is faster than the increase in flow discharge, whereas for $Q > \sim 100 \text{ m}^3/\text{s}$ the decline in flushing duration is not as fast as the increase in discharge. The joint effect of this increasing flow discharge and decreasing duration for $Q > \sim 100 \text{ m}^3/\text{s}$ is the monotonically increasing water volume, implying that a larger flow is associated with a greater flushing efficiency but also a greater amount of water consumption. For example, under the pre-flushing $f_s = 0.24$, the volume of water released for $Q = 100 \text{ m}^3/\text{s}$ is 0.3 km^3 , while the released water volume corresponding to $Q = 200 \text{ m}^3/\text{s}$ is 0.53 km^3 (Figure 8). This 76% increase in water volume results from a 100% increase in discharge and a 12% decline in flushing duration. As pointed out previously, for $Q > \sim 100 \text{ m}^3/\text{s}$ the flushing duration is less sensitive to the flow discharge. In view of the greater water consumption associated with the larger flows (i.e. for $Q > \sim 100 \text{ m}^3/\text{s}$), a smaller flushing discharge might be preferred to minimize gravel loss. The relation between gravel loss and flushing flow is discussed below.

Gravel loss versus flow discharge

The total loss of gravel in the simulation reach is evaluated by summing up the difference between the gravel outflow from sub-reach 3 and the gravel inflow to sub-reach 1 over the entire flushing duration. The relationships between total gravel loss and flushing discharge (Figure 8) reveal that the gravel loss does not monotonically decrease with the flow discharge. Instead, the gravel loss decreases first and then slightly increases with the flow discharge. As the pre-flushing f_s value increases from 0.24 to 0.32, the flow discharge corresponding to the minimum gravel loss decreases from 191 to $135 \text{ m}^3/\text{s}$ (Figure 8). The flushing flows corresponding to the minimum water consumption and gravel loss are given in Figure 9a, where the flows for the minimum water consumption (with an average = $96 \text{ m}^3/\text{s}$) are less variable than those for the minimum gravel loss. Moreover, both the minimum water consumption and gravel loss increase with the pre-flushing f_s value (Figure 9b), implying that higher costs are associated with the greater amount of sand to be removed (i.e. the worse bed sediment condition).

At the end of the previous section, we claimed that for $Q > \sim 100 \text{ m}^3/\text{s}$ a smaller flushing flow might be preferred if that flow also leads to less gravel loss. However, for $Q > \sim 100 \text{ m}^3/\text{s}$ the results (Figure 8) reveal an opposite variation trend of the gravel loss with flow discharge from that of the released water volume (i.e. a smaller flow leads to a greater loss of gravel). This indicates that within a range of flow the released water volume and total gravel loss are two conflicting outcomes of the system. Therefore, it is not possible to simultaneously minimize the gravel loss and water consumption, which raises the need to consider the non-inferior solutions to a problem involving multiple conflicting objectives.

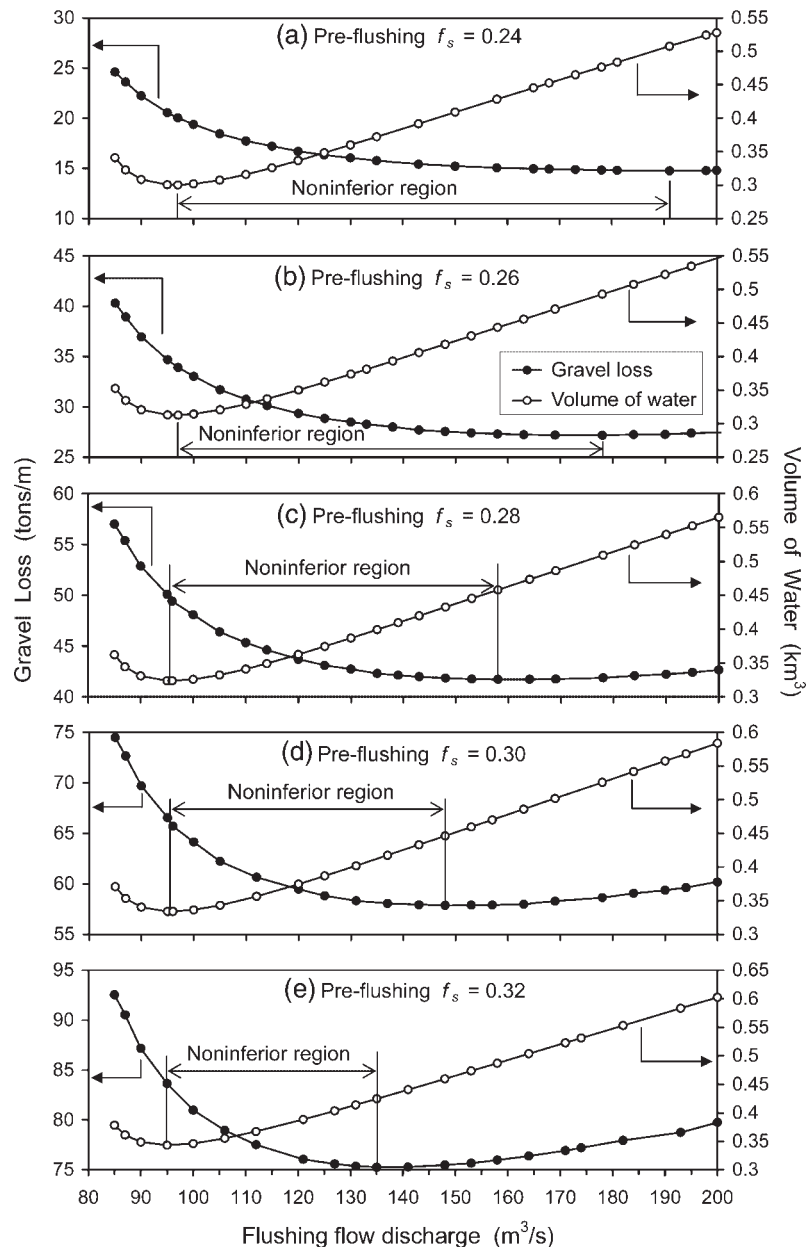


Figure 8. Variations of released water volume and total gravel loss with flushing flow discharge for pre-flushing f_s value: (a) 0.24; (b) 0.26; (c) 0.28; (d) 0.30; (e) 0.32 (non-inferior options in the decision space are demonstrated)

Non-inferior flushing options

The non-inferior option (also known as Pareto optimum) of a multi-objective system is a fundamental concept in the decision-making and policy sciences (Intriligator, 1971). Although a mathematical definition of the non-inferior solution can be found (e.g. Haimes, 1998), here we adopt the qualitative statement (Cohon, 1978) to explain this concept. A non-inferior solution is a feasible solution to which there is no other feasible one that will yield an improvement in one objective without causing degradation to at least one other objective. Specifically, for a solution to be non-inferior, an increase in one objective can be achieved only at the cost of a decrease in some other objective. This solution is obviously not unique. Numerous techniques have been proposed to generate

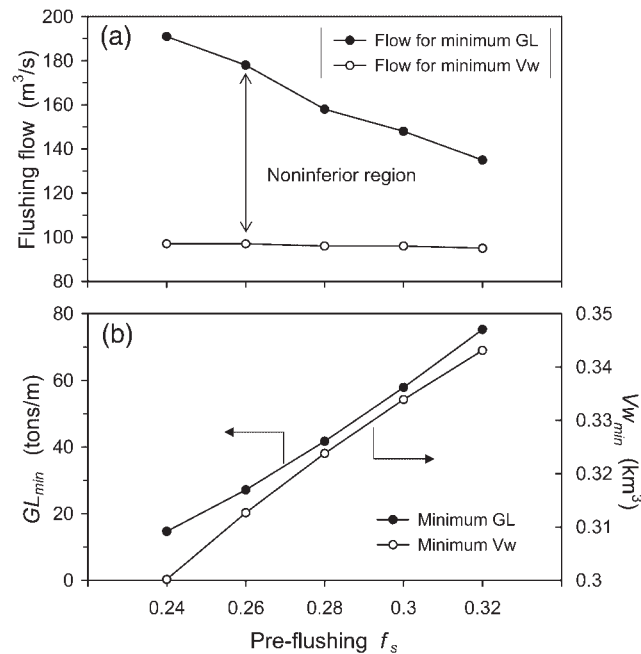


Figure 9. Variations of: (a) flows corresponding to minimum gravel loss and water volume; (b) minimum gravel loss and water volume with pre-flushing f_s value

non-inferior solutions (e.g. reviewed by Cohon, 1978; Chankong and Haimes, 1983; Mays and Tung, 1996). These methods generally require the outcomes of the problem to be expressed as a function of decision and state variables. However, as stated earlier, for the complex system considered in this study, it is difficult to obtain such simple forms of objective function. Nonetheless, the simulation results may be used as a basis for determining the non-inferior options.

It is easily verified that for any two convex curves, such as the ones for water volume and gravel loss (Figure 8), every point between the flows corresponding to the minimum water volume and gravel loss is a non-inferior solution in the decision space. In the non-inferior regions (Figure 8), a decrease in gravel loss is achieved at the cost of an increase in water volume, and vice versa. Out of these regions, the flow options become inferior because the gravel loss and water volume increase simultaneously. It is demonstrated that the non-inferior region becomes smaller for the higher pre-flushing sand content (Figures 8 and 9a), implying that the feasible options are constrained in a narrower range if there is more sand to be removed. Because these non-inferior flows are greater than $\sim 100 \text{ m}^3/\text{s}$, the corresponding flushing durations are less sensitive to the flow discharge, as described previously (Figure 7). For these non-inferior flows the flushing duration may be taken as a less restrictive criterion, thus the original tri-objective system may be simplified as a bi-objective one.

To be more useful, the non-inferior options in the decision space (Figure 8) are transformed to the feasible solutions in the objective space (Figure 10), where the water volume ratio $V_w/V_{w_{min}}$ is defined as the released water volume divided by the minimum water volume, the gravel loss ratio GL/GL_{min} is the total gravel loss divided by the minimum gravel loss ($V_{w_{min}}$ and GL_{min} given in Figure 9b). The results shown in Figure 10 are similar to the Pareto optimal frontiers typically used to demonstrate the non-inferior solutions. Any point on the frontier represents a feasible combination of gravel loss and water volume, and their corresponding non-inferior flushing flow can be found in Figure 8. Figure 10 also quantitatively displays the tradeoffs between the conflicting objectives. For example, under the pre-flushing $f_s = 0.24$, the minimum gravel loss (i.e. for $GL/GL_{min} = 1$) is associated with an extra 69% consumption of water over $V_{w_{min}}$ (i.e. $V_w/V_{w_{min}} = 1.69$). Similarly, minimizing the water consumption (i.e. for $V_w/V_{w_{min}} = 1$) is achieved at a cost of an extra 36% gravel loss over GL_{min} (i.e., $GL/GL_{min} = 1.36$). It is also revealed that the feasible range of system outcomes reduces with the increasing pre-flushing f_s value (Figure 10). For instance, under the pre-flushing $f_s = 0.24$, the feasible ranges of the gravel loss and water volume

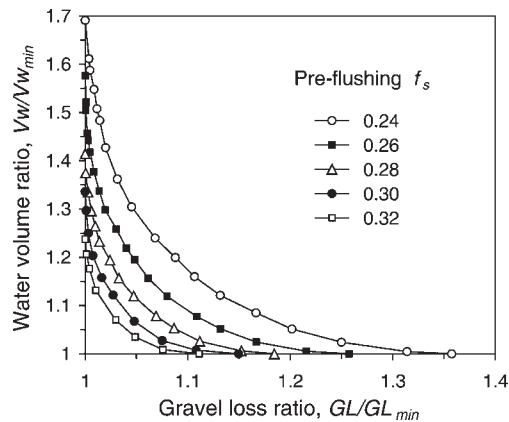


Figure 10. Tradeoffs associated with the feasible combinations of released water volume and total gravel loss under various pre-flushing f_s values (non-inferior options in the objective space are demonstrated)

ratios extend to 1.36 and 1.69, respectively, while under the pre-flushing $f_s = 0.32$, the feasible ranges of these ratios reduce to 1.11 and 1.24, respectively. This, once again, highlights that under a worse bed sediment condition the feasible combinations of released water volume and total gravel loss (or the non-inferior flushing options) are subject to more restrictions.

To further seek the preferred option from the non-inferior solution set, the decision-maker's preference among the multiple objectives, such as the utility function or preferred marginal tradeoff value, must be known (e.g. Mays and Tung, 1996; Haimes, 1998). Searching for the preferred choice of a decision-maker is beyond the scope of this study. Nevertheless, the results presented in Figure 10 provide the decision-maker with useful information about the tradeoffs between conflicting objectives or non-inferior flushing options that can facilitate further analyses.

CONCLUSIONS

In this study we applied the two-fraction sediment routing model to simulate the gravel-sand bed response to flushing flows. This model was specifically developed for the depth flushing process involving the entrainment of surface gravels and the removal of subsurface sands. Parameter values for the Trinity River were used as representative of many gravel-bed rivers. The flushing model was first used to simulate the evolutions of bed composition, bed elevation, and sediment transport rates. The simulation results reveal that the sand cleansing effect propagates from upstream to downstream and from surface to subsurface. For the scenario simulated in this study (i.e. a steady gravel supply from upstream), an equilibrium gravel transport was eventually reached in the simulation reach. The resulting degradation of channel bed implies the potential loss of gravel associated with the release of flushing flows.

The flow-transport system investigated here involves a transient state variable (bed sand content), a decision variable (flushing flow discharge), a flushing goal (ultimate bed sand content), and three objectives to be minimized (flushing duration, released water volume, and total gravel loss). The system outcomes are significantly affected by the pre-flushing sand content, flow discharge, and specified flushing goal. To explore the tradeoffs among these outcomes, a series of numerical simulations were carried out with a range of flows and pre-flushing bed sediment conditions. The results reveal that the flushing efficiency is higher for the greater flow, although the marginal efficiency is much lower for flows $> \sim 100 \text{ m}^3/\text{s}$. For these flows, the flushing duration is less sensitive to variation in flow discharge, thus the original tri-criterion problem may be simplified as a bi-criterion one. It is also revealed that within the non-inferior flow region, gravel loss and water volume are two conflicting outcomes such that a decrease in gravel loss is achieved only at the cost of an increase in released water volume. For the higher pre-flushing sand content, the non-inferior flow region reduces while the minimum water volume and gravel loss increase, implying that under a worse bed sediment condition the feasible flushing options are not only constrained in a narrower range but also associated with higher costs.

The non-inferior options in the decision space are then transformed into the feasible solutions in the objective space. The tradeoffs between the two conflicting outcomes can be quantitatively displayed with such a format. The preferred flushing option can be further selected from these feasible combinations of system outcomes given the decision-maker's preference. The simulation approach presented in this paper has general applicability to other sites, not for the merits of any individual step, some of which are obviously site-specific, but for the manner in which the integrated procedures permit exploration of the non-inferior flushing options and a quantitative analysis of the tradeoffs associated with different flushing flows that is appropriate to the level of data typically available.

ACKNOWLEDGEMENTS

Funding of this study was granted by the National Science Council, Republic of China (NSC 91-2313-B-002-340). The authors acknowledge P. R. Wilcock for his insightful suggestions on an earlier draft of this work. Comments from two anonymous reviewers are appreciated.

REFERENCES

- Andrews ED, Nankervis JM. 1995. Effective discharge and the design of channel maintenance flows for gravel-bed rivers. In *Natural and Anthropogenic Influences in Fluvial Geomorphology*, Costa JE *et al.* (eds). Geophysical Monograph 89. AGU: Washington, DC; 151–164.
- Chankong V, Haimes YY. 1983. *Multiobjective Decisionmaking: A Theory and Methodology*. Elsevier Science: New York.
- Cohon JL. 1978. *Multiobjective Programming and Planning*. Academic Press: New York.
- Haimes YY. 1998. *Risk Modeling, Assessment, and Management*. John Wiley: New York; 197–198.
- Intriligator MD. 1971. *Mathematical Optimization and Economic Theory*. Prentice-Hall: Englewood Cliffs, NJ; 142–177.
- Kondolf GM, Wilcock PR. 1996. The flushing flow problem. *Water Resources Research* **32**: 2589–2599.
- Ligon FK, Dietrich WE, Trush WJ. 1995. Downstream ecological effects of dams, a geomorphic perspective. *Bioscience* **45**: 183–192.
- Mays LW, Tung YK. 1996. Systems analysis. In *Water Resources Handbook*, Mays LW (ed.). McGraw-Hill: New York; 6.1–6.50.
- Milhous RT. 1982. Effect of sediment transport and flow regulation on the ecology of gravel-bed rivers. In *Gravel-bed Rivers*, Hey RD *et al.* (eds). John Wiley: New York; 819–842.
- Reiser DW. 1998. Sediment in gravel bed rivers: ecological and biological considerations. In *Gravel-bed Rivers in the Environment*, Klingeman PC *et al.* (eds). Water Resources Publications: Highlands Ranch, Colo.; 199–228.
- Reiser DW, Ramey MP, Wesche TA. 1989. Flushing flows. In *Alternatives in Regulated River Management*, Gore JA, Petts GE (eds). CRC Press: Boca Raton, Fla.; 91–135.
- Wilcock PR. 1998. Sediment maintenance flows: feasibility and basis for prescription. In *Gravel-bed Rivers in the Environment*, Klingeman PC *et al.* (eds). Water Resources Publications: Highlands Ranch, Colo.; 609–638.
- Wilcock PR, Barta AF, Shea CC, Kondolf GM, Matthews WVG, Pitlick J. 1996a. Observations of flow and sediment entrainment on a large gravel-bed river. *Water Resources Research* **32**: 2897–2909.
- Wilcock PR, Kondolf GM, Matthews WVG, Barta AF. 1996b. Specification of sediment maintenance flows for a large gravel-bed river. *Water Resources Research* **32**: 2911–2921.
- Wu FC. 2000. Modeling embryo survival affected by sediment deposition into salmonid spawning gravels: application to flushing flow prescriptions. *Water Resources Research* **36**: 1595–1603.
- Wu FC, Chou YJ. 2003. Simulation of gravel-sand bed response to flushing flows using a two-fraction entrainment approach: model development and flume experiment. *Water Resources Research* **39**(8): 1211. doi: 10.1029/2003WR002184.